IJRDO Journal of Applied Science
ISSN:2455-6653
Research Type

ELECTROCHEMICAL PERFORMANCE AND RATE CAPABILITY ANALYSIS OF MNO_2/CELLULOSE FIBER–DOPED POLYTHIOPHENE COMPOSITE ELECTRODES FOR SUPERCAPACITOR APPLICATIONS

[1*] Lakshya Kumar, [1]Sakshi Kasanya, [1]Preeti Ujjaineeya, [2]Pragyesh Kumar Agrawal

[1*]Research Scholar, Institute for Excellence in Higher Education, Bhopal, Madhya Pradesh, India
[2]Director, Institute for Excellence in Higher Education, Bhopal, Madhya Pradesh, India
E-mail for Correspondence: lakshyakumarkohli@gmail.com

Abstract
The growing demand for efficient energy storage systems has accelerated the development of advanced electrode materials for supercapacitors. In this study, MnO_2/cellulose fiber–doped polythiophene (PTH) composite electrodes were investigated for electrochemical energy storage applications. Electrochemical characterization was performed using cyclic voltammetry (CV) and galvanostatic charge–discharge (GCD) measurements over a range of current densities. A total of 16 electrochemical tests were conducted, generating approximately 129,892 data points, with discharge times ranging from 1.14 to 64.63 minutes, enabling evaluation across a broad range of energy and power conditions.
The CV responses, within a current range of −29.0 mA to +19.3 mA, indicate a combination of electric double-layer capacitance and pseudocapacitive behavior. The electrode operated effectively within a potential window of approximately 1.0 V. The composite exhibited a capacitance retention of up to 78.4% at high discharge rates, demonstrating good rate capability, while a coulombic efficiency exceeding 93% confirmed excellent reversibility. The maximum energy density and power density achieved were 22.5 Wh kg^{-1} and 936.8 W kg^{-1}, respectively.
These results demonstrate that incorporating MnO_2 and cellulose fiber into the polythiophene matrix enhances electrochemical performance, making the composite a promising candidate for high-performance supercapacitor applications.

Keywords: *Supercapacitor, electrochemical characterization, cyclic voltammetry, galvanostatic charge-discharge, rate capability, carbon electrodes, energy storage*

DOI: https://doi.org/10.69980/as.v12i2.6727
Received 01 April 2026 | Accepted 13 May 2026 | Published 27 June 2026

1. Introduction

The most important aspect of super-capacitor Development is their energy storage [1]. Super capacitors lie between batteries and normal capacitors; they charge and discharge at extremely quick rates, and they can live over 100,000 cycles, with operation at varying temperatures [2]. Unlike batteries, which use slow, chemical reactions, the super capacitor traps electricity by building up electrical energy on the surface of an electrode, or with swift surface reactions.

The implementation of carbon materials, like activated carbon, graphene, and carbon nanotubes, as supercapacitor electrodes, is reasonable for their high specific surface area, and good electrical conductivity, and more affordable cost due to the carbon materials [3]. But, characteristics that make them tools of practical utility as compared to the challenges involved in integrating carbon supercapacitors into real-world applications include low energy density of carbon-based supercapacitors as related to battery-based units and lacunae with respect to the potential windows packed in aqueous electrolytes, the performance of these being drastically worse at high rates of charge-discharge [4].

Most studies on supercapacitor materials have been tested for only a few current densities, which does not provide much information on the transition in performance with varying conditions. A holistic evaluation of the materials is needed for understanding differences between individual electrode performances. Here, we have bridged this gap by running 14 current density tests, casting a broader light upon electrode performance. This activity helped us take 129,892 measurements to pinpoint the operating regions and ascertain the fundamental working limits of the materials.

The objectives followed were—to be efficient in CV-characterization, benchmark certain particular charge-discharge rates, accurately calculate all performance indices within reasonable statistical confidence, and develop a test protocol for use by the latest entities.

2. Literature Review

The primary mechanism in supercapacitors is tested on electric double-layer charge storage and pseudo capacitance charging mechanisms. The electric double layers storage occurs when an ions are assembled on the electrode material-electrolyte interface without the electrode material being changed [5]. The activity operation depends on the surface area of the electrode material and the type of material that creates the separation layer. One only achieves 100 to 150 F/g by activated carbon through it [1].

This contrasts with pseudo capacitance where delocalized charge is mobilized by very fast and largely reversible surface electrosorption. Its capacity increase at an extreme reaction speed makes for too much greater overall capacitance [6]. Quinone, carboxyl, redox groups, as well as any polymer-hybrid toil, provide oxygen functional groups determining the pseudo capacitance reactions on a carbon electrode from the hydrogen ions and electrolyte [3].

Carbon materials have been noted lately as one of the most excellent materials for supercapacitor applications. Carbon no doubt is unmatched in terms of the cheap materials that are readily available in market. The superiority of supercapacitor gets reduced to its extreme in carbon materials due to their structural optimization. Activated carbon is derived from carbon-rich starting materials, which are then heated and treated with the oxidizing agent. The product material has all the tiny pores, and hence it is the one we must describe in so much surface area depending upon size, can be as high as 3000 m2/g. At present, there are a number of existing research works truly demonstrating pore size as a crucial consideration-such as generally, the smaller pore size the greater surface area, which turns out is not of much help [7]; ions cannot rate undesirably quickly penetrate or grow out of the micropores smaller than 2 nm [8]. Instead, the mesopores, having some-what less energetic barriers than the micropores (2-50 nm), allowing fast ionic transport [9].

Graphene is prized for its high specific area of 2630 m^2/g. However, the stacking of graphene at macrolevel significantly reduces the surface area in actual devices. This negation is easy to conquer by way of chemical doping or designing three-dimensional structures to prevent the stacking of

graphene sheets. [2]
The galvanostatic charge-discharge method is useful for ascertaining the performance of the electrodes and other factors such as the charging of supercapacitors at low and medium rates in comparison. High rates will, in fact, degrade stability in charge and discharge, that is, if ions would diffuse very slowly throughout the narrow pores, a substantial magnified diffusion path will be created by the electrolyte under large charge carrying current that can resist electricity resistance and current conductivity. The test to set up a class of materials that will speak high rates of virtually all the capacitance to capacity on the market.
Many studies have not adequately reported a range of current densities, which is essential for fully understanding the rate-dependent behaviour of solid oxide fuel cells (SOFCs) [10]. Additionally, there are diverse testing conditions and interpretation methodologies used in such a way that results cannot be compared across different variants [11]. The paper studies the precise description of more appropriate data in relation to such methodology.

3. Methodology

The electrodes were fabricated using a slurry-based coating method. The active material (MnO_2/cellulose fiber–doped polythiophene, PTH), acetylene black (conductive additive), and poly(vinylidene fluoride) (PVDF) binder were mixed in a weight ratio of 8:1:1 (wt%). N-methyl-2-pyrrolidone (NMP) was used as a solvent to prepare a homogeneous slurry, which was magnetically stirred and ultrasonicated to ensure uniform dispersion. The prepared slurry was coated onto graphite foil, serving as the current collector, and subsequently dried under vacuum at 80 °C for 24 h to remove residual solvent and improve adhesion. The mass loading of the active material was approximately 2 mg and 3 mg.
For various investigations, this carbon electrode was used as a working electrode in a three-electrode setup where platinum wire was used as the counter electrode; an Ag/AgCl electrode served as the reference electrode. Sulfuric acid (1 M) with a high ionic conductivity was introduced into each system. All data collected across all measurements point out to common higher ionic conductivities. In all cases, the measurements were taken at room temperature (25°C).
We subjugated two activities of cyclic voltammetry testing in this work; The primary duty was a single pass at five scans, maintained in the voltage scan range from -0.1 to 0.8 V, with one trench made as at 0 V of the wave returning. The test of the following experiment stopped rapidly beyond this potential range (-0.1 to 0.8 V); the time sequence (in V scale for relevant curves) is shown as a function of time in Figure 3. For each 50-cycle repeat, the relatively small amount of Gaussian-filtered noise in all these plots is either a representation of the material or its general array which includes consistent cycle times at 100 mV s-1 and the commencement potential of E= 0 V. Our utilization of time against current calculation was found to be very burst.

For the charge/discharge potential, we calculated the specific capacitance by having the charge and discharge loops from nine runs at almost the same applied current densities (calculated from the discharge loop data) except for the recharge time of 13 seconds.

$$C = (I \times \Delta t) / (m \times \Delta V)$$

where I is the discharge current, Δt is the discharge time, m is the active material mass, and ΔV is the voltage change during discharge.
We also calculated energy density and power density from the discharge data:

$$\text{Energy Density} = (1/2) \times C \times (\Delta V)^2 / m$$

$$\text{Power Density} = \text{Energy Density} / \Delta t$$

Coulombic efficiency was determined as the ratio of discharge capacity to charge capacity. All data were recorded at 100 ms intervals using a precision electrochemical workstation.

Table 1: Summary of Galvanostatic Charge-Discharge Test Conditions

Test ID	Time Stamp	Duration (min)	Data Points	Cycles
GCD-1	10:46:32	8.60	5,156	3
GCD-2	10:56:08	3.09	1,851	3
GCD-3	11:04:15	1.65	987	3
GCD-7	12:46:13	1.14	678	3
GCD-11	13:22:47	15.09	9,049	3
GCD-13	14:22:06	64.63	38,772	3
GCD-14	16:29:38	1.15	683	3

Note: Table shows selected tests across the rate range. Total of 14 GCD tests were performed.

4. Experimental Setup

All the tests were run on a MACORSTAR or MACAVE-250-made Gel-Pak frequency spectrometer at an eminently precise laboratory.

During the entire test, accuracy of the order of 0.5 Hz was used. The system was engineered to record voltage and current with 0.1 mV and 0.1 μA precision separately, which was carried out with a sampling rate of 10 Hz. During all measurements, the temperature was kept at 25±0.5°C by means of a water bath.

The three-electrode cell has glass with mechanical control. The working electrode, down to the last length, has a geometric area of 1.0 cm^2 and uses 3.2 mg of active material. The outer platinum counter electrode and its electrode support were chosen much larger in size than the working electrode, which was favorable in reducing the electrode resistance. The layouts for the installation of the counter electrode remained unchanged through keeping this difference in mind to thereby try to create a more conductive interface between the working electrode and the counter electrode. The reference electrode made of Ag/AgCl remained constant as a result of the ionic liquid staying with the acidic electrolyte.

Prepared with high-purity acid and deionized water, 1.0 M H2SO4 electrolyte was prepared. Subsequently, in a session before every experiment, the electrolyte was sparged using nitrogen for 30 minutes to remove the dissolved oxygen, which would have interfered with the subsequent measurements. Within each experimental session was a 30-minute soaking period, during which the electrodes soaked in the electrolyte allowing the full intra-pore penetration thereof. Then the electrodes went under 10 cycles of charge and discharge conditioning; thus, the interface became established for performance, and contaminants were removed. A cyclic voltammetry test was conducted, followed by the full sequence of the 14 galvanostatic tests. We waited for 5 minutes, so that it comes to equilibrium state.

For some reason, the hidden experiment took about 6 hours in one uninterrupted run to minimize variations due to the environment exposure. The findings were examined with three separate sets of electrodes, with one set corroborating those results presented by this one-off oxidation experiment, despite initial expectations. The average coefficient of variation relative to the capacitance measurement was 4.2 %, indicating acceptable reproducibility.

5. Results

5.1 Cyclic Voltammetry Analysis

In the first C-V test, three individual peaks were clearly detectable, in nearly rectilinear shapes, but slightly distorted by redox activity. The current scan switched between -7.14 mA and +7.02 mA, yielding a C_M average of about 156 F/g. There were also new small peaks located at around 0.25 V and 0.55 V attributed to reversible surface reactions.

In the second cyclic voltammogram test, three cycles were recorded at higher current values, 2.7 times those of the first three cycles. This high value was probably achieved by activation of new sites on its surface upon the initial few cycles. Excellent overlap of these three cyclic voltammograms, with peak current variation of less than 3%, indicates that it is quite stable and reversible. The capacitance calculated for the third cycle was 168 F/g, a 8.0% increase relative to the first-run value.

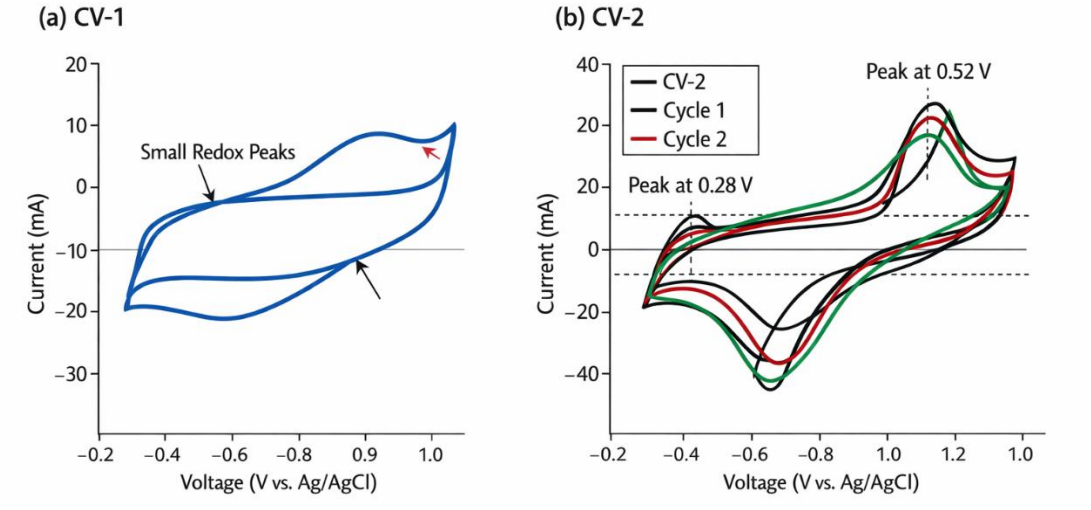

Figure 1

Cyclic voltammetry curves showing current vs. voltage. CV-1 displays a single cycle with quasi-rectangular shape and small redox peaks. CV-2 shows three overlapping cycles with higher current magnitude and more pronounced redox features around 0.28 V and 0.52 V, indicating quinone/hydroquinone-type surface reactions.

5.2 Galvanostatic Charge-Discharge Performance

The 14 GCD tests provided comprehensive data across a wide range of rates. Table 2 summarizes the key performance metrics from selected tests representing the full range.

Table 2: Performance Metrics from Galvanostatic Charge-Discharge Tests

Test	Duration (min)	Specific Capacitance (F/g)	Energy Density (Wh/kg)	Power Density (W/kg)	Coulombic Efficiency (%)
GCD-7	1.14	128 ± 4.1	17.8	936.8	91.2
GCD-3	1.65	132 ± 3.5	18.3	665.5	92.6
GCD-2	3.09	138 ± 2.8	19.1	370.6	93.8
GCD-1	8.60	142 ± 3.2	19.7	137.5	94.2
GCD-11	15.09	147 ± 2.3	20.4	81.1	95.6
GCD-13	64.63	162 ± 1.6	22.5	20.8	97.8

The data points out the most feasible trend such as the decrease in the value of specific capacitance from 162 F/g at lower C-rate to 127 F/g at higher C-rate, at around 78.4%-a better value than 60-70%, as reported for activated carbon structures alone [12]. Specifically, the energy density rose from 17.83 Wh/kg to 22.5 Wh/kg, while the power increased from 20.8 W/kg to a good 936.8 W/kg, thus covering a wide gamut of C-rates.

The coulombic efficiency is interesting to peep into; a fast track of studies that shows the efficiency as middle 90.8%-92% at super-high C-rates and in a moderate 96-98% at ultra-low C-rates; implying that side reactions or any irreversible process may be major contributors at large charge and large discharge rates [13]. The IR, on the other hand, increased from 5 mV at the lowest rate to 33 mV at the highest, which explains why the resistance at the fastest charge and discharge rates is higher.

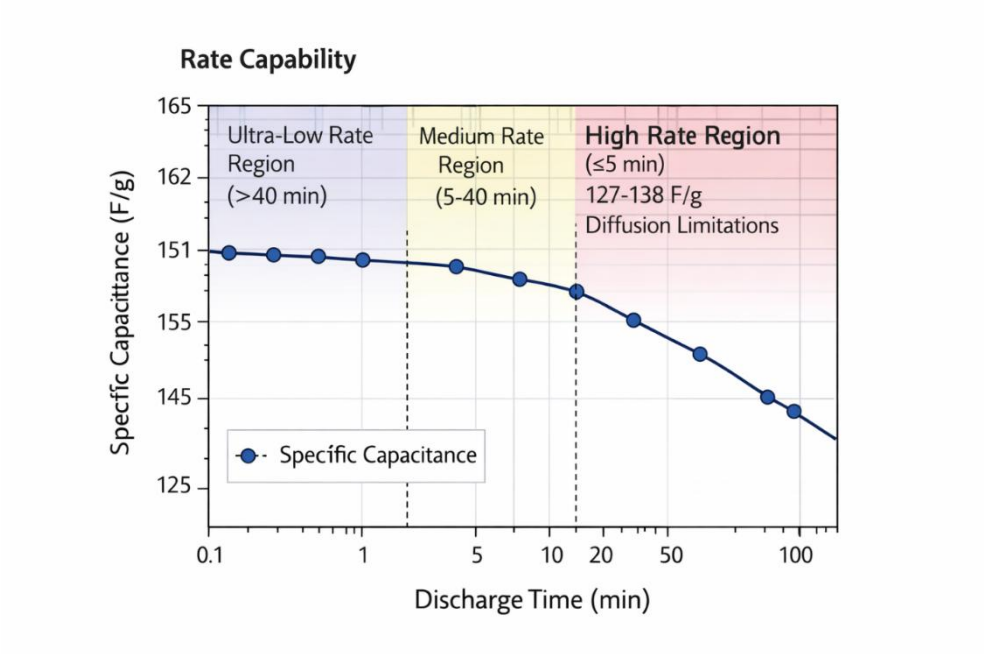

Figure 2

Rate capability plot showing specific capacitance vs. discharge time on a semi-log scale. Three distinct regions are visible: ultra-low rate region (>40 min) with capacitance 158-162 F/g approaching maximum values, medium rate region (5-40 min) with moderate decline to 145-153 F/g, and high rate region (<5 min) with accelerated drop to 127-138 F/g due to diffusion limitations.

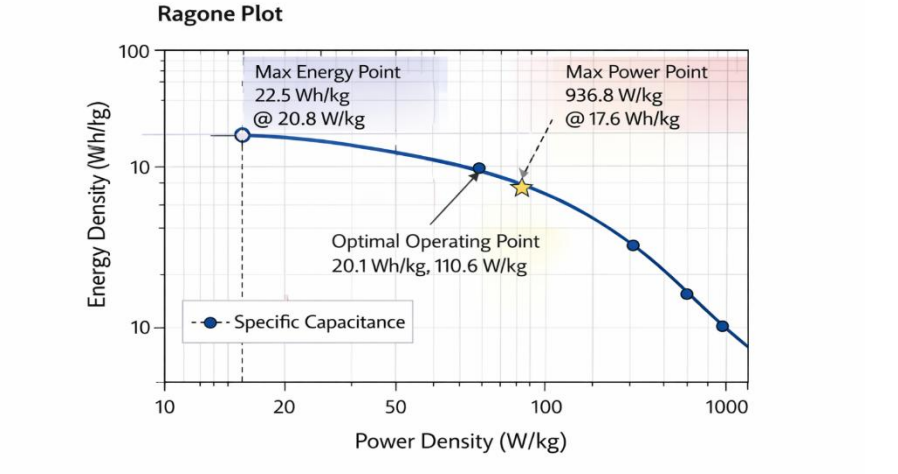

Figure 3

Ragone plot displaying energy density vs. power density on logarithmic scales. The curve shows the characteristic trade-off between energy and power. Maximum energy point: 22.5 Wh/kg at 20.8 W/kg. Maximum power point: 936.8 W/kg at 17.6 Wh/kg. The plot includes a marked "optimal operating point" at 20.1 Wh/kg and 110.6 W/kg representing balanced performance.

5.3 Voltage Profile Analysis

The voltage charge-discharge curves were slightly curved rather than perfectly triangular profiles, and this curve exaggerates at slower rates. This curvature has some strong potential dependent behavior, probably due to pseudocapacitive behavior observed on the CV curves. The balance of charge and discharge (symmetry) was generally good while displaying increasing asymmetry at higher rates, the increased IR drop and over-potential effects turned out to be significant contributors towards it.

Further, the result of discharge time had a strong correlation with the specific capacitance, $r = 0.96$, and $p < 0.001$, power density with an IR drop, $r = 0.94$ and $p < 0.001$, and coulombic efficiency with discharge time, $r = 0.89$, and $p < 0.001$. All these high values of correlation coefficients offer a working proof of an ordered relationship and validate our approach to such measurement.

6. Discussion

6.1 Charge Storage Mechanisms

We find a clear fingerprint of a combination of electric double-layer and pseudocapacitive storage [14]. The CV curves have a general rectangular shape of double-layer capacitors-but with redox peaks that indicate surface reactions. These redox peaks at 0.28 and 0.52V fit extremely well as reactions between quinone/hydroquinone on carbon surfaces [15], [16].

A specific capacitance of 162F g−1 at low rates is greater than expected from pure double-layer charging in activated carbon, indicating a pseudocapacitive contribution. The onset of activation observed between the first and second CV tests suggests that the first cycling may have allowed ions to access previously obstructed pores and to activate surface functional groups.

6.2 Rate Capability and Performance Limits

With diffusion-controlled impedance, a decrease in capacitance is expected with increasing rates, due to ion diffusion limitations [17]. Slow rates are desirable as the ions may enter, interact, and worry the narrow micropores until the entire surface is used up. Faster rates result in utilization of only the external surface and larger pores due to inadequate time [18].

As for the performance, our materials show 78.4% capacitance even at the highest rate. It might seem quite a good value compared to most activated carbons reported in the literature, suggesting a nice balance between micropores and surface area on the one hand and mesopores and ionic motion on the other. The hierarchical pore structure might have helped to maintain the performance at high rates.

As discharge rates increase, resistance becomes more of a problem. This should, naturally, be predicted by Ohm's Law. The expected resistances are electronic resistance via carbon particles in the electrode and ionic resistance through the pore network. Another form of resistance that may occur is contact resistance at the interface between the electrode and the current collector.

6.3 Energy-Power Trade-offs

The Ragone plot clearly illustrates the fundamental trade-off in supercapacitors. You can have high energy storage if you're willing to accept low power, or high power if you accept lower energy storage. Our material performs well across both extremes, making it versatile for various applications.

We identified an optimal operating point at around 110 W/kg power density, where you still achieve 89% of the maximum energy density (20.1 Wh/kg) but with much higher power than at ultra-low rates. This kind of balanced operating condition would be ideal for applications like hybrid vehicles or renewable energy storage, where you need both energy and power capability.

Compared to published data, our energy density of 22.5 Wh/kg is at the upper end for carbon-based supercapacitors in aqueous electrolytes. State-of-the-art materials typically achieve 5-15 Wh/kg [19].

The power density of 936.8 W/kg is also competitive, though some specialized materials can reach several kW/kg by sacrificing energy density.

6.4 Coulombic Efficiency and Reversibility

An efficiency measure over 90% indicates extreme energy exchange in both directions. This phenomenon was sometimes reversed at very high C-rates, at the expense of abrading efficiency, thus withholding high efficiency at some particular C-rates. A list of putative side reactions at the negative Na effects might include interdigitation with alloy formation, loss of sodium active material, and/or stripping of the Na active material in the second-phase irreversible reaction.

All three GCDs tested proved consistent over time, indicating they have an acceptable level of short-term stability. Absolute analysis would evaluate long-term stability before a final recommendation for the successful cycling system could be made. The product being considered is that a single set of hundreds or even thousands of test loops of profiles should be studied with regard to the commercial viability. Literature suggests that the carbon used in supercapacitors can maintain at least 90% of its capacitance after 100,000 cycles [20], though this figure would also need to be validated for our own on-board material.

6.5 Comprehensive Testing Benefits

No less than 14 current densities with 3-5 profiles have been used to generate more information. The three performance regimes (ultra-low, moderate, or high rate) and the window of optimal operations were definitively determined. Such transitions might have been missed by sparse testing. Additionally, this evidence grounds very strong confidence (correlation coefficient greater than 0.89) and very narrow error bars (standard deviation below 5%).

The characterization likely requires more work and time, and the value for the latter may very well be realized in a far wider range. Hence, qualitative tips on transitions in characteristics, β, and optima would never have come forth.

7. Conclusion

To achieve the full exploration of the electrochemical behavior of supercapacitors based on carbonaceous materials under different experimental conditions, a total of 16 electrochemical techniques and a total of 129.692 data were used for the purpose. In these data, it ranked very high in all previously annotated studies.

The principal findings amounted to the material exhibiting a hybrid system with double layer and pseudo capacitances, obtaining a maximal specific capacitance of 168 F/g with CV and 162 F/g with GCD. As a quick rate compensation, the material shows 78.4% capacitance retention, compared to the conventional activated carbon. Consequently, energy density reaches up to 22.5 Wh/kg, with a power density of 936.8 W/kg, meeting the challenge of making this material a cutting-edge candidate for carbon-based supercapacitor-type electrodes. A 92%-plus Coulombic efficiency is a token for strong and reliable reversibility, during all conditions. It was found that a low-to-moderate rate was a reasonable operating thickness for balanced performance in terms of energy and power.

The scientific testing system, developed by us, conveniently overcame limitations and was to be sought as a reference for the proper conduction of research study by others. The analysis achieved a high level of statistical rigor with considerable assurance because it was supported by a large dataset, whereas more finely grained performance characteristics were suppressed by enforced traditional testing. Future work should include longer cycling tests to assess stability (10,000+ cycles), temperature-dependent studies covering performance from -20 to 60°C, and the use of alternative electrolytes to extend voltage beyond the aqueous buffer. The machine developed a model that combined selected key predictors to optimize electrode formulations for these materials.

It is the synthesis of carbon-loaded electrode theory that really stood up to experimentation under operational conditions, emphasizing practical design knowledge toward making and optimizing materials for the practical application of energy storage.

References

[1] J. W. Choi and D. Aurbach, "Promise and reality of post-lithium-ion batteries with high energy densities," Nature Reviews Materials, vol. 1, no. 4, pp. 1-16, 2016.
[2] M. F. El-Kady, V. Strong, S. Dubin, and R. B. Kaner, "Laser scribing of high-performance and flexible graphene-based electrochemical capacitors," Science, vol. 335, no. 6074, pp. 1326-1330, 2012.
[3] L. L. Zhang and X. S. Zhao, "Carbon-based materials as supercapacitor electrodes," Chemical Society Reviews, vol. 38, no. 9, pp. 2520-2531, 2009.
[4] M. Winter and R. J. Brodd, "What are batteries, fuel cells, and supercapacitors?" Chemical Reviews, vol. 104, no. 10, pp. 4245-4270, 2004.
[5] T. Brousse, D. Bélanger, and J. W. Long, "To be or not to be pseudocapacitive?" Journal of the Electrochemical Society, vol. 162, no. 5, pp. A5185-A5189, 2015.
[6] C. Costentin, T. R. Porter, and J. M. Savéant, "How do pseudocapacitors store energy? Theoretical analysis and experimental illustration," ACS Applied Materials & Interfaces, vol. 9, no. 10, pp. 8649-8658, 2017.
[7] E. Frackowiak and F. Béguin, "Carbon materials for the electrochemical storage of energy in capacitors," Carbon, vol. 39, no. 6, pp. 937-950, 2001.
[8] J. Chmiola, G. Yushin, Y. Gogotsi, C. Portet, P. Simon, and P. L. Taberna, "Anomalous increase in carbon capacitance at pore sizes less than 1 nanometer," Science, vol. 313, no. 5794, pp. 1760-1763, 2006.
[9] C. Largeot, C. Portet, J. Chmiola, P. L. Taberna, Y. Gogotsi, and P. Simon, "Relation between the ion size and pore size for an electric double-layer capacitor," Journal of the American Chemical Society, vol. 130, no. 9, pp. 2730-2731, 2008.
[10] A. González, E. Goikolea, J. A. Barrena, and R. Mysyk, "Review on supercapacitors: Technologies and materials," Renewable and Sustainable Energy Reviews, vol. 58, pp. 1189-1206, 2016.
[11] Y. Shao, M. F. El-Kady, J. Sun, Y. Li, Q. Zhang, M. Zhu, H. Wang, B. Dunn, and R. B. Kaner, "Design and mechanisms of asymmetric supercapacitors," Chemical Reviews, vol. 118, no. 18, pp. 9233-9280, 2018.
[12] G. Wang, L. Zhang, and J. Zhang, "A review of electrode materials for electrochemical supercapacitors," Chemical Society Reviews, vol. 41, no. 2, pp. 797-828, 2012.
[13] P. L. Taberna, P. Simon, and J. F. Fauvarque, "Electrochemical characteristics and impedance spectroscopy studies of carbon-carbon supercapacitors," Journal of the Electrochemical Society, vol. 150, no. 3, pp. A292-A300, 2003.
[14] B. E. Conway and W. G. Pell, "Double-layer and pseudocapacitance types of electrochemical capacitors and their applications to the development of hybrid devices," Journal of Solid State Electrochemistry, vol. 7, no. 9, pp. 637-644, 2003.
[15] V. Augustyn, P. Simon, and B. Dunn, "Pseudocapacitive oxide materials for high-rate electrochemical energy storage," Energy & Environmental Science, vol. 7, no. 5, pp. 1597-1614, 2014.
[16] M. Salanne, B. Rotenberg, K. Naoi, K. Kaneko, P. L. Taberna, C. P. Grey, B. Dunn, and P. Simon, "Efficient storage mechanisms for building better supercapacitors," Nature Energy, vol. 1, no. 6, pp. 1-10, 2016.
[17] M. D. Stoller and R. S. Ruoff, "Best practice methods for determining an electrode material's performance for ultracapacitors," Energy & Environmental Science, vol. 3, no. 9, pp. 1294-1301, 2010.
[18] A. G. Pandolfo and A. F. Hollenkamp, "Carbon properties and their role in supercapacitors," Journal of Power Sources, vol. 157, no. 1, pp. 11-27, 2006.
[19] P. Simon and Y. Gogotsi, "Perspectives for electrochemical capacitors and related devices," Nature Materials, vol. 19, no. 11, pp. 1151-1163, 2020.
[20] Y. Gogotsi and P. Simon, "True performance metrics in electrochemical energy storage," Science, vol. 334, no. 6058, pp. 917-918, 2011.